American Mineralogist, Volume 82, pages 878–887, 1997

Surface site-specific interactions of aspartate with calcite during dissolution: Implications for biomineralization

H. Henry Teng and Patricia M. Dove

School of Earth and Atmospheric Sciences, Georgia Institute of Technology, Atlanta, Georgia 30332-0340, U.S.A.

Abstract

Calcite occurs widely as a mineral component in the exoskeletons and tissues of marine and freshwater invertebrates. Matrix macromolecules involved in regulating the biological growth of calcite in these organisms are known to share a carboxylic-rich character that arises from an abundance of the acidic amino acids aspartate (Asp) and glutamate (Glu). This study determines the interactions of Asp with calcite $\{10\bar{1}4\}$ faces during dissolution using in situ fluid-cell atomic force microscopy (AFM) and macroscopic ex situ optical methods. In control experiments, etch-pit morphologies produced by dissolution in simple undersaturated solutions reflect the inherent symmetry of the $\{10\bar{1}4\}$ faces with a rhombus form. With the introduction of Asp, surface site reactivities are modified to yield isosceles triangular etch pits and hillocks. With continued exposure to Asp-bearing solutions, these triangular pits coalesce and the surface evolves into a network of interconnected tetrahedral etch hillocks. The component tetrahedral ''sides'' have Miller-Bravais indices of (0001), $(\bar{1}101)$, and $(0\bar{1}11)$. These faces intersect the $(10\bar{1}4)$ face in the [010], $[45\bar{1}]$, and $[\bar{4}11]$ directions to compose the three edges of the triangular etch pits. Structural and stereochemical contraints suggest that the $(\bar{1}101)$ and $(0\bar{1}11)$ faces in the hillock are a combination of corresponding faces from the $\{\bar{1}102\}$ and $\{\bar{1}100\}$ crystallographic forms.

Results of this dissolution study are consistent with previous growth experiments showing that Asp causes preferential development of the {0001} and possibly the $\{\bar{1}100\}$ forms of calcite. These observations support mechanisms proposing that the new forms are stabilized by the molecular recognition of Asp functional groups for specific surface sites. Because Asp stabilizes identical faces during growth and dissolution, we suggest that dissolution studies offer an alternative means of determining the crystal forms that develop during biomineralizing processes and a more direct means of identifying those surface sites involved. We demonstrate that the stability of crystallographic directions expressed by step edges is controlled by the relative reactivities of surface sites. Our findings yield new insights into surface structure controls on mineral reactivity.

Introduction

Biomineralization is the process by which the biologically mediated activities of organisms lead to mineral nucleation and growth. This process has been divided into two fundamentally different types based on the degree of biological control (Lowenstam 1981). In biologically controlled mineralization, morphologically complex structures nucleate and grow in concert with a genetically programmed macromolecular matrix of proteins, polysaccharides, and lipids. The resulting mineral microarchitectures fulfill specific physiological functions such as the addition of stiffness and strength to skeletal tissues (e.g., Berman et al. 1993; Mann 1993). These ''biomaterials'' can also have remarkable physical properties that cannot be imitated by the most sophisticated synthetic materials (Vincent 1990). In contrast, biologically induced mineralization occurs as a result of interactions between the biological activities of an organism and its surrounding physical environment to produce secondary mineral precipitation. These minerals lack known biological function (Skinner 1993). In this type of biomineralization, biological systems exercise little direct control over mineral formation although biological surfaces may be important in the induction of processes. At least 60 carbonate, phosphate, oxide, sulfate, and sulfide minerals can be formed through biomineralizing activities (Simkiss and Wilbur 1989). Of these, the calcium carbonates, calcite and aragonite, have the most widespread occurrence and form through either type of biomineralization.

Previous studies of organic-calcite interactions

Several studies have investigated processes governing biomineralization by examining calcite growth morphologies produced in the presence of proteins, amino acids, and other organic compounds. The matrix macromolecules involved in regulating biological growth of carbonate minerals share an acidic character created by an abun-

0003–004X/97/0910–0878$05.00

dance of the amino acids aspartate (Asp) and glutamate (Glu) (Crenshaw 1972; Weiner et al. 1983; Weiner 1986; Addadi et al. 1987; Lowenstam and Weiner 1989). In vitro studies suggest that these macromolecules modify calcite morphology by selectively binding to certain crystal faces and inhibiting growth (Addadi and Weiner 1985; Addadi et al. 1987; Berman et al. 1988; Mann et al. 1990; Berman et al. 1995). When adsorbed onto a solid substrate, they induce the formation of unusual crystallographic faces such as (0001). For example, Addadi and Weiner (1985) and Addadi et al. (1987) demonstrated that Asp-rich proteins and β-sheet polyaspartate adsorbed on sulfonated polystyrene surfaces lead to the formation of calcite (0001) growth faces. Berman et al. (1988) observed that the acidic macromolecules extracted from sea urchin tests stabilized prismatic faces. Mann et al. (1990) found that α-aminosuccinate (aspartate) and γ-carboxyglutamate were more efficient at stabilizing (promoting the formation of) first-order prismatic $\{\bar{1}100\}$ faces than second-order prismatic {1100} growth faces. They also showed that amino-functionalized carboxylates (amino acids) are more effective than their simple carboxylic acid counterparts at stabilizing the formation of these new faces. These observations suggest that acidic amino acids influence growth through the orientation and interaction of their side-chain carboxylates with calcite surfaces and their ability to create extended Ca-interacting domains. Thus, surface-specific interactions of growth modifiers are believed to be an essential controlling factor in development of diverse morphologies for the minerals in biological systems.

These investigations of mineral formation in solutions containing diverse organic constituents remind us that we lack a consistent mechanistic model that can describe and predict the interactions of organic compounds with mineralizing surfaces. This continuing gap in our scientific knowledge also hinders our ability to predict or control carbonate precipitation and growth in other natural or engineered systems where organic compounds are present. However, the literature contains clues suggesting that a consistent framework for a mechanistic model exists. Previous biomineralization studies suggest that a combination of electrostatic, stereochemical, and geometric recognition processes occur between organic molecules and mineral surfaces during crystal growth (Mann 1988). Although this hypothesis is largely drawn from ex situ SEM examinations of crystals taken from growth solutions, it suggests an underlying principle: The geometry and chemistry of functional groups that characterize acidic amino acids have highly specialized interactions with specific surface site types. If true, it may be possible to unravel the mechanisms governing ''recognition'' processes in a systematic and predictable way.

Approach of this study

With the development of fluid-cell techniques in atomic force microscopy (AFM), we begin to determine the nature of these specialized interactions through in situ observations of nanoscale reaction processes. Fluid-cell AFM records the evolution of mineral surface microtopography, individual step heights, and relative rates of step migration as they occur in aqueous solutions. Previous studies demonstrate the utility of AFM for understanding calcite surface structures and reactivity. AFM has been used to investigate calcite growth and dissolution processes, to observe the formation or retreat of the mono-molecular layer 3 Å steps on the $(10\bar{1}4)$ cleavage surfaces (Hillner et al. 1992a, 1992b; Gratz et al. 1993; Dove and Hochella 1993; Stipp et al. 1994) and to study the configuration of molecular-scale surface structures (Ohnesorge and Binnig 1993; Stipp et al. 1994). This paper continues the investigation of controls on carbonate surface reactivity by examining the influence of Asp on calcite microtopography.

Aspartate-calcite interactions are the focus of our study because of the documented importance of this system to biomineralization. Previous studies report the influence of Asp on calcite growth using ex situ macroscopic approaches, but none has determined the microscopic controls of this amino acid on growth or dissolution by in situ microscopic methods. Recognizing that experiments using the monomeric form of aspartic acid do not duplicate the Asp residue found in natural proteins, we investigated the crystallographic-specific interactions of Asp with calcite surfaces with the goal of answering the following questions: (1) How does Asp modify the surface topography of calcite during dissolution? (2) Is it possible to identify the site-specific interactions of organic growth modifiers through studies of dissolution? (3) Do similar surface-specific interactions occur during growth and dissolution to stabilize development of the same crystal faces? Answers to these questions are a first step in our long-term goal of characterizing the controls of complex organic compounds on mineral formation in biomineralization.

The use of dissolution studies as a tool for determining crystal symmetry is well documented in mineralogy and crystallography (e.g., Zoltai and Stout 1984; Putnis 1992) and materials science (e.g., Sangwal 1987). In a similar study, Honess and Jones (1937) suggested that etch morphology expresses the symmetry of both the substrate crystal and the solvent by comparing etch patterns obtained using optically inactive and active solvents on different crystallographic faces of carbonate minerals in detail. Etching has also found applications in separating enantiomorphous conglomerates and assigning the absolute configuration of polar and chiral compounds (Shimon et al. 1986). However, we are unaware of studies using dissolution or other chemical-etching methods to probe the mechanisms by which additives modify the relative reactivities of surface sites with similar structures. In this dissolution study, we investigate the nature of Asp interactions with calcite surface sites by combining in situ microscopic observations of variations in etch pit morphologies developed in real time with ex situ examination of surface topographies produced after long-term expo-

sure to aspartate. We show that sites along specific crystallographic directions become less reactive during dissolution in the presence of Asp and new surfaces that were previously unstable are formed. These surfaces are the same as those developed in Asp-modified growth experiments. This discovery suggests that mineral dissolution studies using suites of selected amino acids and organic compounds may help to unravel the mechanisms by which organic compounds mediate the nucleation and growth of minerals in biological systems.

Experimental procedures

Sample and solution preparation

The calcite samples were obtained from a single large crystal of optical-quality Iceland spar. Each experiment began by cleaving a new fragment from this crystal to obtain a fresh $(10\bar{1}4)$ surface. Fragments were handled with tweezers to avoid surface contamination by skin oils and were cleaned with small bursts of N_2(g) to remove small particles and dust adhering to the surfaces. Samples used in fluid cell AFM experiments had dimensions of approximately $5 \times 5 \times 1$ mm^3. Each fragment was mounted onto a steel puck using sealing wax. Larger samples with dimensions of $15 \times 15 \times 3$ mm^3 were prepared for the macroscopic optical analyses. These fragments were mounted on glass slides using sealing wax to cover all faces but one for an exposed area of approximately 15×15 mm^2.

Aspartate (Asp) in the L-monosodium form [Na-$OOCCH_2CH(NH_2)COOH$] was used in our experiments. The Asp molecule is a two-C chain that has a carboxyl and an amine group (zwitterionic moiety) attached to one C and a carboxyl group attached to the other as a side chain. The carboxylate groups have pK_a values of 1.99 and 3.9 associated with the zwitterion and the side chain, respectively (Voet and Voet 1995). The pK_a value of the amine group is approximately 10. Stock solutions of 10^{-2} and 10^{-1} M Asp were prepared using bio-research grade deionized water (resistivity greater than 18 megohm-cm, total organic C less than 10 ppb). These solutions were equilibrated with air before use and the pH of all solutions was measured to be approximately 5.6. Thus, the Asp molecule had fully ionized carboxylate groups and a protonated amine group at the pH of our experiments.

Imaging by fluid contact AFM

AFM experiments were conducted using a Nanoscope III scanning probe microscope (Digital Instruments) equipped with an E-sized piezoelectric scanner (maximum scan area of 14×14 μm^2). Surfaces were imaged using commercially available Si_3N_4 cantilevers having a triangular shape, length of 200 μm, and force constant of approximately 0.6 N/m. Radii of lever tips were approximately 30–50 nm, which corresponds to a theoretical contact force of $27–46 \times 10^{-9}$ N between tip and sample (Eggleston 1994). To reduce the possibility of artificial changes in microtopography by tip-surface interactions, the interactive force was minimized by tuning the force calibration curve. Scan rates ranged from 5 to 9 Hz with 512 sampling points per scan line, which corresponds to capture times of 1–2 min per image. The equilibrium imaging temperature was approximately 30 °C because of thermal energy created by the laser and microscope body (Dove and Chermak 1994). Minimal thermal drift of the scanner was observed.

The fluid cell used in these AFM experiments had an internal volume of 50 μL and a flow-through capability that permits solutions to pass continuously through the reaction chamber. See Dove and Chermak (1994) for a description of cell design. The mounted samples were first imaged in air to locate a relatively flat area and to optimize image quality. Then solutions were manually injected into the fluid cell using a syringe. After wetting the cell and surfaces, a peristaltic pump was used to maintain a constant flow of solution through the cell at a maximum pumping rate of 0.8 mL/h.

Treatment of the surface examined by ex-situ dissolution

The samples prepared for long-term etching (see previous section) were placed in a flow-through chamber with a fluid volume of 20 mL. Over a period of two weeks, a peristaltic pump circulated 500 mL of 0.01 and 0.1 M Asp solutions through the chamber at a rate of 20 mL/h. Using optical microscopy, progressive etching of the surface was monitored daily. At the end of this period, the samples were removed from solution and dried with small bursts of N_2 gas. Macroscopic observations of the resulting etched surfaces were examined using a Leica Quantimet Q-570 digital image analyzer coupled to an optical microscope. Incident illumination was used to obtain optimal contrast of surface features and the images were stored as digital files.

Observations

Development of etch features in deionized water

Within a few seconds of injecting deionized water into the fluid cell, AFM discerned the development of dissolution etch pits with near-perfect rhombus symmetry on the calcite $(10\bar{1}4)$ face. Figure 1 shows a typical AFM image of a calcite surface exposed to distilled water for less than 2 min. Surfaces were relatively flat with a maximum topographic relief of approximately 30 Å. Individual 3 Å steps were observed over the imaging area, and the terraces between adjacent steps were atomically flat. The shape of these etch pits is consistent with previous studies reporting the dissolution of calcite in water (Hillner at al. 1992a, 1992b; Stipp et al. 1994).

For each new experiment, we used the orientations of etch pits developed in water to establish the nanoscale crystallographic orientation of fragments. Gratz et al. (1993) and Stipp et al. (1994) have shown that pit edges (and thus step edges) correspond to the $[\bar{4}41]$ and $[48\bar{1}]$ directions as illustrated in Figure 1. This orientation allowed us to make direct comparisons with subsequent

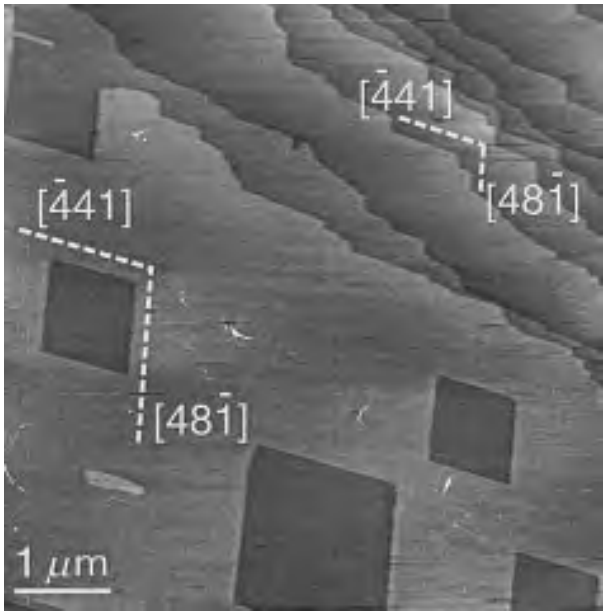

FIGURE 1. Fluid-cell AFM image of a (10$\bar{1}$4) calcite crystal face reacting with deionized water shows the etch features produced after two minutes of dissolution. The individual steps are monomolecular units having a height of 3 Å. The pit edges and step edges reveal the [$\bar{4}$41] and [48$\bar{1}$] crystallographic directions that develop in simple inhibitor-free solutions and thus disclose the nanoscale orientation of the calcite fragment. The maximum topographic relief of this surface is about 30 Å.

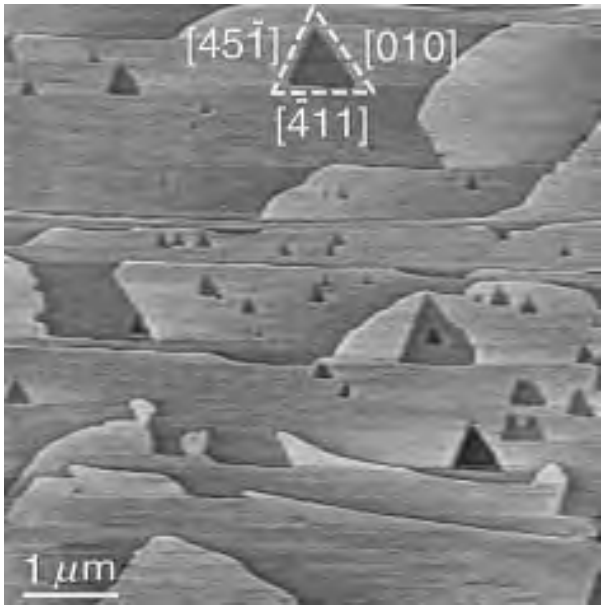

FIGURE 2. Fluid-cell AFM image of the same area of the (10$\bar{1}$4) face shown in Figure 1 after exposure to 10^{-1} M Asp solution for 10 min. The rhombus-shaped etch pits were removed during continued dissolution and triangular pits formed. The three sides of the pits correspond to the [010], [45$\bar{1}$], and [$\bar{4}$11] directions and step heights are approximately 3 Å.

observations of pit development with the introduction of aspartate.

Transition in etch pit morphology with introduction of aspartate

After establishing the crystallographic orientation of each new fragment in deionized water, the input solution was changed to 10^{-2} or 10^{-1} M Asp. Within a few tens of seconds, the introduction of aspartate solutions promoted a sharp transition in the dissolution features to yield etch pits having a triangular morphology. Figure 2 illustrates the triangular surface structures that typically developed over 10 min of exposure to a 10^{-1} M aspartate solution (for the same area shown in Fig. 1). None of the three step edges forming these triangular pits was parallel to the pit edge directions observed in Figure 1. Rather, they revealed new crystallographic directions: [010], [45$\bar{1}$], and [$\bar{4}$11]. The edge lengths of triangles shown in Figure 2 varied from a few to 500 nm, illustrating that the pit morphology was not a function of pit size. The angles between step edges composing the pits are approximately 64° between [45$\bar{1}$] and [41$\bar{1}$], and 58° between [45$\bar{1}$] and [010], and [41$\bar{1}$] and [010] directions.

Figures 3a–3d record the transition from rhomboid to triangular pits that resulted when the input solution was changed from a 0 to 10^{-1} M Asp solution. Figure 3a shows the characteristic etch features produced during short-term exposure to distilled water. Intermediate Figures 3b and 3c show the evolution of surface structures that occurs with the introduction of aspartate. Figure 3b was collected over an imaging time of 56 s (scan rate of 9 Hz) and records a sharp contrast between the water-dissolved surface (upper part of image) and Asp-reacted surface (lower part). The scratchy center portion of this image corresponds to a 14 s transition period during which the solution was changed from 0 to 10^{-1} M Asp as a step input. This occurred while the cantilever was disturbed by the uneven flow of injecting a pulse of the new solution. The last 18 s of Figure 3b (lower part of image) recorded the early stage of triangular pit development. Newly developed pits with sizes as small as a few tens of nanometers already bore a triangular-like shape, but the directions of step edges were irregular. Figure 3c shows that, after another minute, the [$\bar{4}$41] and [48$\bar{1}$] crystallographic directions that were stable during dissolution in water were hardly discernible. Yet, only two of the three triangular pit edges, [45$\bar{1}$] and [$\bar{4}$11], had clearly developed during this period. A comparison of Figures 3b and 3c showed that while Asp promotes a transition in dissolution surface structure within seconds, the rate of development of the [010] direction is slower. Rather, this third edge continued to display the two components of the previously dominant [$\bar{4}$41] and [48$\bar{1}$] directions, and the [010] edge was still not fully stabilized after another two minutes as indicated in Figure 3d, which shows the almost fully developed triangular pits. In repeated experiments, we found that the transition from

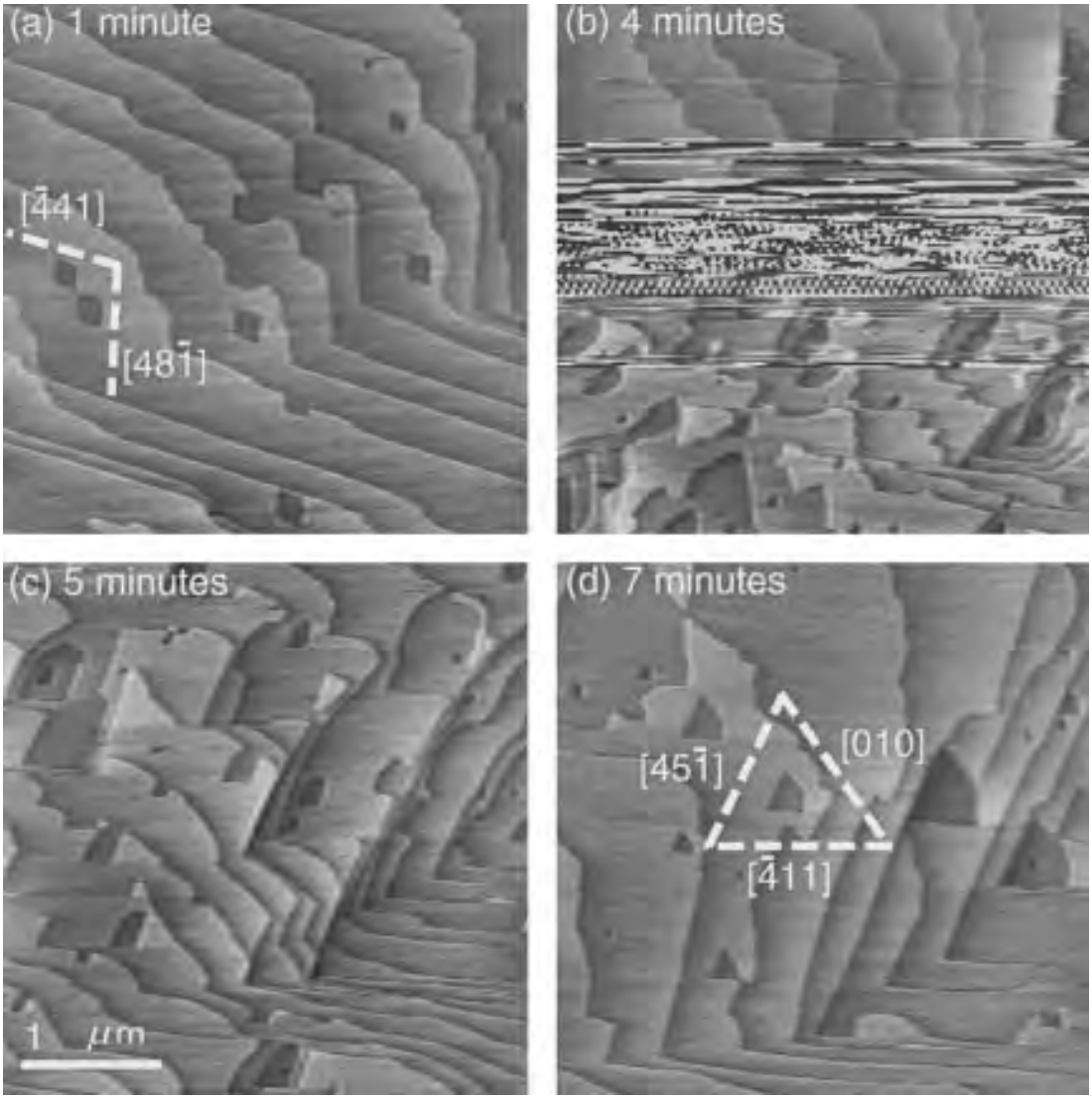

FIGURE 3. A time sequence of AFM images showing the transition from rhombus to triangular etch-pit morphology. Each image was collected over a 56 s period. (**a**) Time = 1 min. The ($10\bar{1}4$) face in deionized water results in formation of rhombus-shaped etch pits. (**b**) Time = 4 min. Transition from deionized water (upper portion of image) to 10^{-1} M Asp solution (lower portion of image) shows that Asp immediately interacts with the calcite surface to modify etch-pit morphologies. The central ''scratchy'' portion of image corresponds to the 14 s period when input solution was changed. (**c**) Time = 5 min. The [$45\bar{1}$] and [$\bar{4}11$] directions have clearly developed, but triangular form is incomplete. (**d**) Time = 7 min. Triangular morphology is nearly complete but the pit edges corresponding to the [010] direction continue to have curvature. Incomplete development of the [010] relative to the [$45\bar{1}$] and [$\bar{4}11$] directions suggests that surface sites along [010] have a weaker interaction with Asp or perhaps form at a slower rate. Continued reaction leads to formation of the isosceles features shown in Figure 2.

a rhombus to triangular etch-pit morphology was readily reversible when the input solution was returned to water.

Development of etch hillocks with long term exposure to aspartate solutions

Examining the calcite samples that were continuously exposed to 0.1 M Asp solutions in a flow-through chamber for two weeks also revealed the development of triangular pits. These pits were so extensive that interconnected tetrahedral etch hillocks had developed as residual features from the formerly flat ($10\bar{1}4$) cleavage surface. Figure 4 shows a typical surface that developed over an area of approximately 3×3 mm^2. Sizes of the hillocks, as measured by the side length of their base triangles, ranged from a few micrometers to several hundred micrometers.

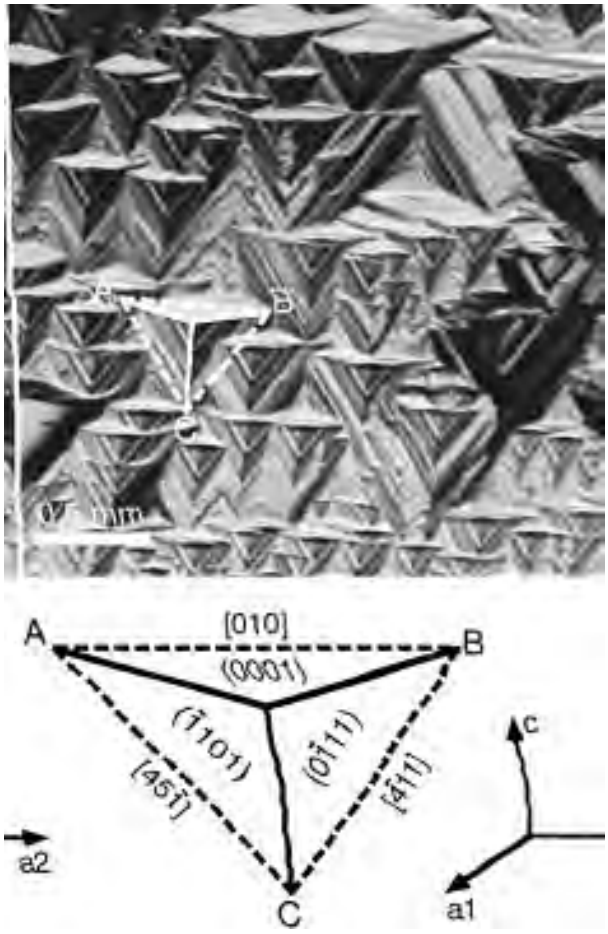

FIGURE 4. Digital image of etch hillock features developed on the $(10\bar{1}4)$ face after etching in 10^{-1} M Asp solution for two weeks. The new surface is characterized by well-oriented tetrahedral etch hillocks that are interconnected by triangular etch pits. The labels show the directions of the three component faces composing the tetrahedrons and the directions of individual layers composing the hillocks. The corresponding crystallographic axes are also shown.

Because the fragments used in these ex situ dissolution experiments were sufficiently large to determine the crystallographic orientation mechanically, we were able to ascertain the crystallographic directions of the hillock slopes. Using image analysis, we found that the slopes of each hillock corresponded to the calcite (0001), $(\bar{1}101)$, and $(0\bar{1}11)$ faces. Thus, the 3 Å steps, which represent the monomolecular steps of the original $(10\bar{1}4)$ face, were the triangular layers within each hillock. These layers intersect the (0001) face at the [010] axis, the $(\bar{1}101)$ face at the $[45\bar{1}]$ axis, and the $(0\bar{1}11)$ face at the $[\bar{4}11]$ axis. Recall that these directions are parallel to pit edges observed in the AFM experiments.

DISCUSSION

The formation of triangular etch pits on the cleavage rhombohedron of calcite by contact with aspartate solution was first reported in the macroscopic etch experiments by Honess and Jones (1937). However, we are only beginning to understand Asp-calcite surface interactions.

The mechanism by which aspartate promotes the development of {0001} and $\{\bar{1}101\}$ forms can be understood in terms of the calcite structure and the nature of aspartate-surface interactions. First, the crystal structure of calcite (point group $\bar{3}^2/m$) is often described as alternating planes of Ca atoms and CO_3 groups. These planes are perpendicular to the *c* axis (e.g., Fig. 5) and constitute the basal {0001} form. Individual carbonate groups within a plane are also perpendicular to the *c* axis, but they are rotated in adjacent carbonate planes in a staggered conformation. Thus, only the basal {0001} faces bear a threefold rotational symmetry. For a detailed description of the calcite structure see Reeder (1983) and references therein. The {0001} is also unusual in comparison to other forms because it possesses a strong electrical dipolar moment induced by single component layers (pure Ca or pure CO_3). Because the charge on (0001) faces cannot be fully neutralized by underlying atoms (of opposite charge), surfaces consisting of the {0001} form are less stable than those faces that lack this dipolar character. This lack of stability is in agreement with the theoretical analysis of Titiloye et al. (1993).

Second, the ability of aspartate to modify calcite surface site reactivities can be examined in terms of the relative surface complexation strength of ligands in solution. In the presence of H_2O, Stipp and Hochella (1991) and Van Cappellen et al. (1993) have shown that surface-bound Ca atoms form >Ca-OH complexes by a reaction that can be represented as:

$$>Ca^+ + H_2O \leftrightarrow >Ca\text{-}OH + H^+ \quad (1)$$

where ">" indicates a surface-bound Ca atom. With the introduction of aspartate, Reaction 1 competes with the >Ca-Asp complexation reaction:

$$>Ca^+ + Asp^- \leftrightarrow >Ca\text{-}Asp. \quad (2)$$

Although the complexation constant for surface Reaction 2 is unknown, we infer that the binding constant of Reaction 2 is significantly greater than that of Reaction 1 by analogy with the relative strengths of comparable aqueous complexation constants (e.g., Schindler and Stumm 1987). The aqueous complexation reaction:

$$Ca^{2+} + Asp \leftrightarrow Ca^{2+}\text{-}Asp(aq) \quad (3)$$

has a relatively strong pK_a of 1.6 (Chaberek and Martell 1959) compared to the association of H_2O with Ca ion by the reaction:

$$Ca^{2+} + H_2O \leftrightarrow Ca\text{-}OH(aq) + H^+ \quad (4)$$

which has a pK_a value of 12.85 (e.g., Stumm and Morgan 1981). Thus, the pK_a value of Reaction 3 is approximately ten orders of magnitude greater than that of Reaction 4, which suggests that the >Ca-Asp complex in Reaction 2 may also be the predominant surface species when aspartate molecules are present in solution. This is signifi-

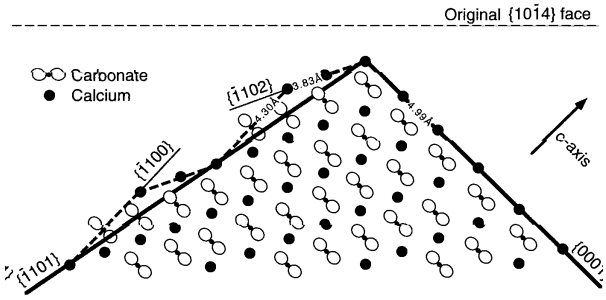

FIGURE 5. Schematic cross-sectional view of the calcite structure showing the crystallographic forms developed in the presence of Asp from the initial {10$\bar{1}$4} cleavage surface. The {0001} and {$\bar{1}$102} forms are single component layers of pure Ca atoms or CO_3 groups but differ from each other in the orientation of planar CO_3 groups and atomic spacings (see discussion). In contrast, the {$\bar{1}$100} form has equal numbers of Ca and CO_3. Solid lines indicate the {0001} and {$\bar{1}$101} forms that become stabilized upon the introduction of Asp to develop the tetrahedral etch hillocks shown in Figure 4. Dashed lines represent the combination of {$\bar{1}$102} and {$\bar{1}$100} forms to yield the pseudo {$\bar{1}$101} form.

cant because the stronger interaction of Asp with the surface can inhibit the hydrolysis of >Ca sites during dissolution (see later discussion) by at least two mechanisms: (1) The larger physical size of the aspartate molecules in comparison with inorganic aqueous ions can limit the approach of H_2O molecules to the hydrolyzing calcite-water interface (e.g., Conway 1981). (2) The formation of a >Ca-Asp surface complex reduces the rate or frequency of hydrolysis reactions (e.g., see discussion in Dove and Czank 1995, and references therein). Hence, portions of the calcite surface that are Ca rich or structurally well-matched to the aspartate stereochemistry are protected or preferentially stabilized by Asp.

Mechanism for development of the {0001} form

As discussed earlier, the {0001} form does not develop in simple aqueous solutions but rather becomes stabilized with the introduction of Asp. Expression of {0001} on the (10$\bar{1}$4) cleavage face is necessarily constrained by the orientation of its pure Ca layer with respect to the dissolution surface. Figures 2 and 3 show that within each 3 Å layer on the (10$\bar{1}$4) face, one side of each triangular pit forms by preferentially stabilizing sites lying along the [010] direction. The [010] direction is significant because it is the line formed by the intersection of the cleavage surface plane with the single component layer of Ca atoms or CO_3 groups composing the {0001} form. As Asp binds with Ca atoms exposed along the [010] direction, one side of each pit becomes a ''stack of edges'' parallel to [010]. Continued dissolution leads to a (0001) face as the pit deepens. With extensive dissolution, the pits enlarge and merge to form the residual hillocks illustrated in Figure 4. One slope on each hillock corresponds to the {0001} form.

This mechanism suggests that Asp stabilizes {0001} solely by electrostatic interactions of the lone carboxyl group with the pure Ca layer. The other carboxyl of the zwitterion is less likely to play a role because its negative charge is partially neutralized by the adjacent NH_3^+ group. Our findings and the study of Rajam and Mann (1990) indicate that stereochemical and geometric recognition mechanisms do not play a significant role in {0001} development.

Mechanism for development of the {$\bar{1}$101} form

The orientations of residual hillocks in Figure 4 show that Asp also stabilizes the equivalent ($\bar{1}$101) and (0$\bar{1}$11) faces. In contrast to the basal {0001} form, these faces are composed of equal numbers of Ca and CO_3 groups and hence are not dipolar. The mechanism for the development of this form is not readily apparent as adjacent cation and anion sites within the ($\bar{1}$101) and (0$\bar{1}$11) planes are separated by nearly 8 Å to result in a low surface-packing density. Also, adjacent Ca sites in the planes are separated by nearly 16 Å. Each of these distances is greater than the length of single aspartate molecule, which suggests that neither face is stabilized by the binding of carboxyl groups to surface sites in these planes. Thus, crystallographic and organic stereochemical constraints indicate that pure ($\bar{1}$101) and (0$\bar{1}$11) faces cannot form.

These considerations lead us to propose that the ($\bar{1}$101) and (0$\bar{1}$11) faces that occur as two slopes forming the macroscopic residual hillocks in Figure 4 are the result of stabilizing alternating segments of the (1$\bar{1}$02) and ($\bar{1}$100), and the (01$\bar{1}$2) and (01$\bar{1}$0) faces at a microscopic scale. The ($\bar{1}$102) and (01$\bar{1}$2) faces belong to the {$\bar{1}$102} form of calcite. Similar to {0001}, faces in {$\bar{1}$102} are also composed of pure Ca (or pure CO_3) layers. Stabilization of this form by Asp can be attributed to the same electrostatic mechanism that promotes development of the basal face (see previous section). However, extensive development of {$\bar{1}$102} does not appear to be permitted. This may be understood by comparing the structure of the {0001} and {$\bar{1}$102} forms. The latter has a higher density of Ca atoms or CO_3 groups composing the surface layer (and thus, a still-higher dipole moment). For example, the schematic illustration in Figure 5 shows that the distance between adjacent Ca atoms in the {$\bar{1}$102} form is only 3.83 Å compared to approximately 4.99 Å for the {0001} form. This results in a Ca surface density that is 70% greater. The result of this greater dipole moment is to limit stabilization of {$\bar{1}$102} to small areal scales. As seen in Figure 5, crystallographic structure dictates that the shortest segment of atoms that can form along this plane is approximately 8 Å long.

Although our investigation cannot estimate a critical length (or area) above which {$\bar{1}$102} is destabilized, one can see that the dipole moment associated with this form can be reduced by the formation of the intermittent prismatic face segments illustrated in Figure 5. Unlike {0001} and {$\bar{1}$102}, the faces composing the prismatic {$\bar{1}$100} form are not dipolar. However, previous studies propose that a combination of electrostatic, geometric,

and stereochemical recognition processes between calcite surfaces and Asp molecules can stabilize the prismatic form. Mann et al. (1990) stated that recognition occurs by cooperative electrostatic interactions of the carboxyl and amine groups of the zwitterion with >Ca atoms and $>CO_3$ groups in adjacent layers of the $\{\bar{1}100\}$ form. These surface groups make unique bidentate binding sites because the cations and anions are separated by 3.3 Å. This is equal to the distance between the amino and carboxyl groups of the Asp zwitterionic moiety ($^+H_3NCH_2COO^-$). This matching also allows sufficient space to position the α-C near the surface because CO_3 groups on the $\{\bar{1}100\}$ form are oriented so that only one O atom "protrudes" (Mann et al. 1990). This binding configuration enables the remaining $-CH_2COO^-$ group to replace a CO_3 position in the adjacent anion layer. The overall geometric and stereochemical cooperativity results in Asp binding on the $\{\bar{1}100\}$ calcite faces in a linear pattern. We suggest that development of $\{\bar{1}100\}$ during dissolution in the presence of Asp occurs by the same recognition processes proposed by Mann et al. (1990).

Our AFM images have insufficient microscopic resolution to prove that $(\bar{1}101)$ and $(0\bar{1}11)$ are a combination of the corresponding faces in the $\{1\bar{1}02\}$ and $\{\bar{1}100\}$ forms by direct observation. For example, Figure 2 shows a 5.86 × 5.86 μm² area as a composite of 512 × 512 pixels of data. Thus, each pixel covers an area of nearly 13 023 Å² or a length of approximately 114 Å, which is 10–15 times greater than the length of segment represented in Figure 5. However, two lines of experimental evidence support this model. First, only the projection of the {0001} and $\{\bar{1}101\}$ forms onto the $(10\bar{1}4)$ face can explain the isosceles triangular features shown in Figure 2. This projection yields angles of 63°, 58°, and 58° between the three step edges, which is consistent with our experimental observations. The previous discussion indicates that the likely explanation for development of $\{\bar{1}101\}$ is an average expression of the $\{\bar{1}100\}$ and $\{\bar{1}102\}$ forms. A second piece of evidence is suggested by examining the etch hillock slopes in Figure 4. In contrast with the very smooth (0001) faces expressed on the hillocks, the $(\bar{1}101)$ and $(0\bar{1}11)$ faces are uneven as evidenced by the alternating light-dark patterns. This suggests that neither of these surfaces are true crystallographic faces.

Our findings support the previous study by Titiloye et al. (1993) indicating that the magnitude of the dipole moment on a crystal face is central to modifying electrostatic interactions and stabilizing individual faces. We postulate that a still-stronger driving force is needed to overcome the greater dipole moment on the $\{\bar{1}102\}$ form to slow the hydrolysis rate of groups within this plane and fully stabilize the formation of the corresponding $(\bar{1}102)$ and $(0\bar{1}12)$ faces expressed by the hillocks. This is supported by our experimental observations that {0001} did not develop when Asp concentrations were $\leq 10^{-2}$ M. At lower concentrations, we speculate that the quantity of negatively charged Asp molecules was insufficient to modify the hydrolysis of surface sites on {0001} relative to sites on the $\{10\bar{1}4\}$ faces.

One possible means of fully stabilizing the $\{\bar{1}102\}$ faces would be the use of a still-higher concentration of Asp. However, we were not able to test this without exceeding the solubility of the calcium aspartate salt. Another possibility is the use of a compound that has additional recognition properties between the organic and inorganic components at the interface. This was accomplished by Berman et al. (1995) by nucleating calcite onto a substrate matrix of 10,12-pentacosadiynoic acid (a 25-C chain carboxylic acid). Their observation of $\{\bar{1}102\}$ formation led to a model using cooperative alignment of calcite components with carboxyl groups at the mineral-organic interface in addition to electrostatic interactions with the $>Ca^+$ surface sites.

Significance to understanding interactions of other amino acids with calcite

Our findings suggest that amino acids with chemical and physical structures similar to aspartate may modify calcite reactivities in growth and dissolution by similar mechanisms. Glutamate is the only naturally occurring amino acid that shares the acidic character of Asp. A macroscopic study by Honess and Jones (1937) demonstrated that Glu also affects the etch morphology of calcite.

This paper is not intended to address the kinetics of calcite dissolution in Asp solutions, but we can make qualitative observations regarding the influence of Asp on dissolution and growth rates. First, we see that the interactions of Asp with calcite do not render surface sites nonreactive. Sites along the [010], $[45\bar{1}]$, and $[\bar{4}11]$ directions become less reactive relative to those along other directions. Yet, Figure 3 shows that step edges visibly retreat in Asp-bearing solutions at a rate of several hundred nanometers per minute. We predict that rates of growth or dissolution in comparable Glu and Asp solutions should be similar because of their similar interaction strengths. Second, the continued migration of steps suggests that Asp is a relatively weak inhibitor compared to phosphate ion, a well-documented strong inhibitor. AFM observations of Dove and Hochella (1993) showed that all step migration ceases with the introduction of a 10 μM PO_4^{3-} solution. Thus, bulk dissolution rates in PO_4^{3-}-bearing solutions should be significantly slower than in Asp solutions.

Although amino acids are simplistic analogs for the complex proteins present in organic-rich environments, our observations suggest that a systematic growth or dissolution study using a suite of selected amino acids could be used to unravel the mechanisms by which their functional groups interact with surfaces and allow us to quantify their controls on growth or dissolution kinetics. By investigating the influence of neutral side chains, polar uncharged side chains, charged side chains, and others in simple systems, we may develop a mechanistic frame-

work for solute-surface interactions that govern the formation of different mineral polymorphs and their morphologies in biological systems.

Determining surface controls of other inhibitors on etch morphology

It is generally accepted that the shapes and orientations of etch pits developed on crystallographic faces correspond to the projection of the point group symmetry of that crystal onto the individual crystal face concerned (e.g., Zoltai and Stout 1984; Sangwal 1987; Putnis 1992). Our findings show that this rule-of-thumb holds even in solutions in which specialized surface interactions modify the etch morphology. More specifically, the glide plane symmetry on the $(10\bar{1}4)$ face is unaffected by the change in activity of surface sites. However, our results demonstrate that the sites that control the development of the $[\bar{4}11]$ and $[48\bar{1}]$ directions in water become less reactive compared to those sites that lead to the formation of $[45\bar{1}]$, $[\bar{4}11]$, and [010] directions when Asp is introduced. This suggests that the stability of steps along particular crystallographic directions is controlled by the relative reactivities of surface sites. Thus, we show that compounds having specialized interactions with the surface can yield new insights into controls on mineral reactivity.

Dissolution experiments as a tool in biomineralization studies

The results of this dissolution study are consistent with previous growth experiments showing that Asp causes preferential development of the {0001} and possibly the $\{\bar{1}100\}$ forms of calcite (e.g., Addadi and Weiner 1985; Mann et al. 1990). This suggests that dissolution experiments may offer an alternative means of identifying the crystal face that forms and a more direct means of identifying those sites involved in stabilizing each new face. Dissolution experiments have the advantages of being less difficult and less time-consuming to conduct than growth studies. Yet, further study is needed to determine if etching features produced in the presence of inhibitors during dissolution can be general indicators of the faces that become stabilized during mineral growth. If future studies find this holds true, dissolution studies may become a useful tool to determine the site-specific interactions of many different biological compounds with mineral surfaces and to improve our understanding of the physical processes governing biomineralization.

Acknowledgments

This work was supported by the Basic Energy Sciences Program of the U.S. Department of Energy through grant number DE-FG05-95-ER14517. We thank Dirk Bosbach, Kathryn Nagy, and an anonymous reviewer for helpful comments during review. We also thank Rich Reeder for careful review of calcite crystallography during the final editorial handling.

References cited

Addadi, L. and Weiner, S. (1985) Interaction between acidic proteins and crystals: Stereochemical requirements in biomineralization. Proceedings of the National Academy of Sciences 82, 4110–4114.

Addadi, L., Moradian, J., Shay, E., Maroudas, N.F., and Weiner, S. (1987) A chemical model for the cooperation of sulfates and carboxylates in calcite crystal nucleation: relevance to biomineralization. Proceedings of the National Academy of Sciences 84, 2732–2736.

Berman, A., Addadi, L., and Weiner, S. (1988) Interactions of sea-urchin skeleton macromolecules with growing calcite crystals: A study of intracrystalline proteins. Nature, 331, 546–549.

Berman, A., Hanson, J., Leiserowitz, L., Koetzle, T.F., Weiner, S., and Addadi, L. (1993) Biological control of crystal texture: a widespread strategy for adapting crystal properties to function. Science, 259, 776–779.

Berman, A., Ahn, D.L., Lio, A., Salmeron, M., Reichert, A., and Charych, D. (1995) Total alignment of calcite at acidic polydiacetylene films: cooperativity at the organic-inorganic interface. Science, 269, 515–518.

Chaberek, S., and Martell, A.E. (1959) Organic sequestering agents. Wiley, New York.

Crenshaw, M.A. (1972) The soluble matrix from Mercenaria mercenaria shell. In H. K. Erben, Ed., Biomineralization research reports: International Symposium on Problems in Biomineralization 6, p. 6–11. Schattaure Verlag, Stuttgart.

Conway, B.E. (1981) Ionic Hydration in Chemistry and Biophysics. Studies in Physical and Theoretical Chemistry 12, 773 p. Elsevier, Amsterdam.

Dove, P.M. and Chermak, J. (1994) Mineral-water interactions: Fluid cell applications of scanning force microscopy. In K.L. Nagy and A.E. Blum, Eds., CMS Workshop Lectures: Scanning Probe Microscopy of Clay Minerals, 139–170 p. Clay Minerals Society, Washington, DC.

Dove, P.M. and Czank, C.A. (1995) Crystal chemical controls on the dissolution kinetics of the isostructural sulfates: Celestite, anglesite, and barite. Geochimica et Cosmochimica Acta, 59, 1907–1915.

Dove, P.M. and Hochella, M.F., Jr. (1993) Calcite precipitation mechanisms and inhibition by orthophosphate: In situ observations by Scanning Force Microscopy. Geochimica et Cosmochimica Acta, 57, 705–714.

Eggleston, C.M. (1994) High-resolution scanning probe microscopy: Tip-surface interaction, artifacts, and applications in mineralogy and geochemistry. In K.L. Nagy and A.E. Blum, Eds., Scanning Probe Microscopy of Clay Minerals. CMS workshop lectures, p. 3–90. Clay Minerals Society, Washington, DC.

Gratz, A.J., Hillner, P.E., and Hansma, P.K. (1993) Step dynamics and spiral growth on calcite. Geochimica et Cosmochimica Acta, 57, 491–495.

Hillner, P.E., Manne, S., Gratz, A.J., and Hansma, P.K. (1992a) AFM images of dissolution and growth on a calcite crystal. Ultramicroscopy, 42–44, 1387–1393.

Hillner, P.E., Gratz, A.J., Manne, S., and Hansma, P.K. (1992b) Atomic scale imaging of calcite growth and dissolution in real time. Geology , 20, 359–362.

Honess, A.P. and Jones, J.R. (1937) Etch figure investigations with optically active solvents. Bulletin of the Geological Society of America, 667–722.

Lowenstam, H.A. (1981) Minerals formed by organisms. Science, 211, 1126.

Lowenstam, H.A. and Weiner, S. (1989) On Biomineralization, p. 21–24. Oxford University Press, Oxford.

Mann, S. (1988) Molecular recognition in biomineralization. Nature, 332, 119–124.

———(1993). Molecular tectonics in biomineralization and biomimetic materials chemistry. Nature, 365, 499–505.

Mann, S., Didymus, J.M., Sanderson, N.P., Heywood, B.R., and Aso Samper, E.J. (1990) Morphological influence of functionalized and nonfunctionalized α, ω-dicarboxylates on calcite crystallization. Journal Chemical Society Faraday Transaction, 86, 1873–1880.

Ohnesorge, F. and Binnig, G. (1993) True atomic resolution by atomic force microscopy through repulsive and attractive forces. Science, 260, 1451–1456.

Putnis, A. (1992) Introduction to Mineral Sciences, 206 p. Cambridge University Press, Cambridge.

Rajam, S. and Mann, S. (1990) Selective stabilization of the (001) face

of calcite in the presence of lithium. Journal Chemical Society Chemistry Communications, 1990, 1789.

Reeder, R.J. (1983) Crystal chemistry of the rhombohedral carbonates. In Mineralogical Society of America Reviews in Mineralogy, 11, 1–47.

Sangwal, K. (1987) Etching of Crystals: Theory, experiment, and application. North-Holland, Amsterdam.

Schindler, P.M., and Stumm, W. (1987) The surface chemistry of oxides, hydroxides, and oxide minerals. In W. Stumm, Ed., Aquatic surface chemistry, p. 83–110. Wiley, New York.

Shimon, L.J.W, Lahav, M., and Leiserowitz, L. (1986) Stereoselective etchants for molecular crystals. Resolution of enantiomorphs and assignment of absolute structure of chiral molecules and polar crystals. Nouveau Journal De Chimie, 10, 723–737.

Simkiss, K. and Wilbur, K.M. (1989) Biomineralization- Cell Biology and Mineral Deposition, 43 p. Academic Press, San Diego.

Skinner, H.C. (1993) A review of apatites, ion and manganese minerals and their roles as indicators of biological activity in black shales. Precambrian Research, 61, 209–229.

Stipp, S.L. and Hochella, M.F., Jr. (1991) Structure and bonding environments at the calcite surface as observed with X-ray photoelectron spectroscopy (XPS) and low energy electron diffraction (LEED). Geochimica et Cosmochimica Acta, 55, 1723–1736.

Stipp, S.L., Eggleston, C.M., and Nielsen, B.S. (1994) Calcite surface structure observed at microtopographic and molecular scales with atomic force microscopy (AFM). Geochimica et Cosmochimica Acta, 58, 3023–3033.

Stumm, W. and Morgan, J.J. (1981) Aquatic Chemistry, 243 p. Wiley, New York.

Titiloye, J.O., Parker, S.C., and Mann, S. (1993) Atomic simulation of calcite surfaces and the influence of growth additives on their morphology. Journal of Crystal Growth, 131, 533–545.

Van Cappellen, P., Charlet, L., Stumm, W., and Wersin, P. (1993) A surface complexation model of the carbonate mineral-aqueous solution interface. Geochimica et Cosmochimica Acta, 57, 3505–3518.

Vincent, J. (1990) Structural Biomaterials, 244 p. Princeton University Press, Princeton, New Jersey.

Weiner, S. (1986) Organization of extracellularly mineralized tissues: A comparative study of biological crystal growth. CRC Critical Review in Biochemistry, 20, 365.

Weiner, S., Traub, W., and Lowenstam, H.A. (1983) Organic matrix in calcified exoskeletons. In P. Westbroek and E.W. de Jong, Eds., Biomineralization and biological metal accumulation, p. 205–224. Reidel, Dordrecht.

Voet, D. and Voet, J.G. (1995) Biochemistry (2nd ed.), p. 58–59. Wiley, New York.

Zoltai, T., and Stout, J.H. (1984) Mineralogy: Concepts and Principles, 58 p. Macmillan, New York.

Manuscript received September 12, 1996
Manuscript accepted May 28, 1997